Published in final edited form as:
Dev Dyn. 2009 April ; 238(4): 875–886. doi:10.1002/dvdy.21910.

KIT AND *foxd3* GENETICALLY INTERACT TO REGULATE MELANOPHORE SURVIVAL IN ZEBRAFISH

Cynthia D. Cooper[1,*,#], **Tor H. Linbo**, and **David W. Raible**
Department of Biological Structure, University of Washington, Seattle WA 98195

Abstract

We have investigated the role of *foxd3* activity in conjunction with signaling by the *kit* tyrosine kinase receptor in zebrafish black pigment cell (melanophore) development. As loss-of-function of these molecules individually has distinct effects on melanophore number, we have examined the phenotype of double mutants. Individuals with a null mutation in *kit* have fewer melanophores than wildtype, with cells lost through death. When *kit* mutants are injected with *foxd3* antisense morpholino oligonucleotides or crossed with a *foxd3* zebrafish mutant, they have more melanophores than their uninjected or *foxd3*+ counterparts. Examination of *foxd3* loss-of-function in two additional *kit* mutants that differentially alter *kit*-dependent migration and survival indicates a change in melanophore number in survival mutants only. Consistently, TUNEL analysis confirms a partial rescue of melanophores from cell death. Ectopic expression of *foxd3* indicates that *foxd3* promotes early melanophore death only when *kit* is inactive. Taken together, these data suggest a *kit*-dependent role for *foxd3* in the regulation of melanophore survival.

Keywords

melanophore; survival; morphology; kit signaling; foxd3; neural crest; zebrafish

INTRODUCTION

Early during vertebrate development, cells localized to the lateral neural plate boundary respond to extrinsic signals inducing them to become a transient, migratory population of cells, the neural crest. Upon their induction, neural crest cells respond to extrinsic and intrinsic cues to promote their terminal differentiation into several distinct cells types, including pigment cells, glia, neurons of the dorsal root ganglia and cartilage of the facial bony structures (for a recent review see Sauka-Spengler and Bronner-Fraser, 2006). Neural crest and resulting derivatives have not only become an intriguing model for understanding mechanisms controlling cell fate decisions and migration, but also for examining the events important for lineage survival once fate decisions are made.

Neural crest derived melanocytes (melanophores in fish and frogs) are providing extensive insight into mechanisms promoting lineage survival (Cooper and Raible, 2008). Several genes, including Kit tyrosine kinase receptor (Kit), Bcl-2, MAPK, ADAMTS20 and Mitf have been implicated in melanocyte survival (Geissler et al., 1988; Hodgkinson et al., 1993; Opdecamp et al., 1997; Dorsky et al., 1998; Lister et al., 1999; Parichy et al., 1999; Takeda

[*]Corresponding author: Cynthia D. Cooper (cdcooper@vancouver.wsu.edu).
[#]Current address: School of Molecular Biosciences, Washington State University, Vancouver, 14204 NE Salmon Creek Avenue, Vancouver, WA 98686-9600, Phone: 360-546-9342, Fax: 360-546-9064, cdcooper@vancouver.wsu.edu
1959 NE Pacific Street, Health Sciences Building G-520, Mailstop 357420, Seattle WA 98195-7420, Phone: 206-616-1048, Fax: 206-543-1524

et al., 2000; McGill et al., 2002; Widlund et al., 2002; Dunn et al., 2005; Silver et al., 2008). The latter four genes function downstream of *kit* signaling (Geissler et al., 1988; Hodgkinson et al., 1993; Opdecamp et al., 1997; Dorsky et al., 1998; Lister et al., 1999; Parichy et al., 1999; Takeda et al., 2000; McGill et al., 2002; Widlund et al., 2002; Dunn et al., 2005; Silver et al., 2008). Originally identified as a key factor in mouse melanogenesis, hematopoeisis and primordial germ cell development (Geissler et al., 1988; Copeland et al., 1990; Bernex et al., 1996), Kit signaling is also essential for embryonic melanophore survival in zebrafish (Parichy et al., 1999). *kit*^{b5} mutant zebrafish have a reduction in *kita* activity. A second *kit* orthologue, *kitb*, is not expressed in pigment cells (Mellgren and Johnson, 2005); to avoid confusion with previous studies, hereafter we will refer to the *kita* gene as *kit*. In *kit* mutants, melanophores are initially specified and differentiate, but are reduced in number as compared to wildtype zebrafish. Furthermore, the majority of melanophores fail to leave sites of origin and undergo apoptosis, most evident between 5 and 6 days post-fertilization (dpf;Parichy et al., 1999). Zebrafish mutagenesis screens have allowed the identification of novel melanophore survival genes, including *touchtone* and TRPM7, which function in distinct pathways to regulate maintenance of the melanophore lineage (Cornell et al., 2004; McNeill et al., 2007). Additionally, loss of *kit* function in zebrafish is not lethal (this study; Parichy et al., 1999). Thus, zebrafish melanophores are a resource for discovering novel survival genes as well as genes functioning to modulate *kit* signaling.

Both loss- and gain-of-function studies in chick and zebrafish have uncovered functions for *foxd3* in black pigment cell development. Specifically, chick melanocytes are strongly affected by *foxd3* loss-of-function, as this promotes an increase in the percentage of melanocytes developing in neural crest explant culture. Overexpression of *foxd3* leads to inhibition of chick melanogenesis (Kos et al., 2001). Intriguingly, loss of zebrafish *foxd3* activity leads to distinct effects on the onset of melanogenesis. Delays in *mitfa* expression and melanoblast migration are observed in the *foxd3* zebrafish mutants, *mother superior* (*mos188*) and *foxd3*^{zdf10}, yet the number of melanophores is similar to wildtype by day 3 and 5, respectively (Montero-Balaguer et al., 2006; Stewart et al., 2006). Examination of morpholino oligonucleotide (MO) mediated loss-of-function in zebrafish shows more subtle changes in expression patterns of melanophore markers (Lister et al., 2006; Ignatius et al., 2008). These seemingly conflicting results may suggest subtle differences in the *foxd3* protein level, activity or temporal requirements necessary to mediate Foxd3 function. Consistently, other forkhead transcription factor family members, such as FoxO1 and FoxO3, show a high degree of post-translational modification in response to *kit* signaling, critical to their intracellular localization and subsequent effects on regulating cell survival (Engstrom et al., 2003). Whether *foxd3* is similarly regulated or regulated via alternative genetic mechanisms remains poorly understood.

As loss of *foxd3* or *kit* activity have opposing effects on zebrafish melanophore location and numbers, we hypothesized that *foxd3* may modulate *kit* function. To test the relationship between *foxd3* and *kit* signaling in melanophore development, we investigated the effect of *foxd3* loss-of-function on melanophores in multiple zebrafish *kit* mutants. Our evidence suggests *foxd3* loss-of-function modifies melanophore morphology and numbers when the survival function of the *kit* receptor is defective. Consistently, TUNEL analysis indicates a rescue of *kit* negative melanophores when *foxd3* activity is reduced. Last, melanophore specification from neural crest and cell differentiation are largely unaffected by *foxd3* MO injection. Our data suggest *foxd3* and *kit* signaling oppose each other in the survival of embryonic melanophores and may cooperate to establish proper melanophore patterning and number.

RESULTS

kit^{w34} has defects in *kit* dependent melanophore migration and survival

Zebrafish melanophores are sensitive to *kit* loss-of-function as characterized with the *kit* null mutant, *kit*^{b5} (previously known as *sparse*; Johnson et al., 1995; Parichy et al., 1999). *kit*^{b5} mutants display defects in melanophore migration and survival, and also show fewer melanophores than wildtype zebrafish. We have isolated a mutant, *kit*^{w34} that has defects in melanophore migration and survival, similar to *kit*^{b5}. Homozygous *kit*^{w34} larvae show substantial cell loss by 4 dpf, and migration away from sites of origin to peripheral locations in the anterior region of the head, lateral stripe and ventral stripe are all defective (Fig. 1A and 1B). Analysis of 6dpf progeny resulting from a *kit*^{w34}/*kit*^{b5} cross indicate similar defects in melanophore migration, morphology and survival as observed in each homozygous allele alone (Fig. 1C–1E). Lack of *kit* message at 23 somite stage (Fig. 1F and 1G) and exclusion of *kit* exon 10 in *kit*^{w34} genomic DNA (data not shown) further support the notion that *kit*^{w34} harbors a null mutation in the *kit* tyrosine kinase receptor gene.

We also examined the effects of *kit*^{w34} loss-of-function on adult pigment pattern. Similar to homozygous *kit*^{b5} mutants (Parichy et al., 1999), we see a reduction in overall pigmentation in *kit*^{w34} adults (Fig. 1H and 1I). In fish with wildtype pigmentation, dark stripes consist of melanophores, intermingled with shiny silver iridophores and occasional xanthophores (Parichy and Turner, 2003). The lighter, interstripes consist of iridophores and yellow xanthophores, with melanophores diffusely dispersed throughout the scales. In *kit*^{w34} mutant adults, the dark stripes are present, but lighter and less organized than those found in wildtype adults (Fig. 1I, arrowhead). In addition, dorsally positioned melanophores are largely missing in the skin, scales and dorsal fin (Fig.1H and I, arrow). Thus, similar to *kit*^{b5} mutants, *kit*^{w34} mutant zebrafish illustrate the requirement for *kit* signaling in melanophore maintenance and adult pigment pattern.

Inhibition of *foxd3* activity partially rescues melanogenesis in *kit* null mutants

Little is known regarding the factors involved in generating specificity with *kit* signaling. Using *kit*^{w34} mutants, we looked for genetic modulators of *kit* function, with the goal of identifying molecules involved in transducing or blocking *kit* signals. Studies in chick and zebrafish suggest a role for forkhead transcription factor *foxd3* in inhibition of melanogenesis (Kos et al., 2001; Montero-Balaguer et al., 2006; Stewart et al., 2006). Furthermore, additional evidence indicates changes in melanophore distribution in 5 dpf *foxd3* null zebrafish mutants (*foxd3*^{zdf10}; Stewart et al., 2006), suggesting a role for *foxd3* in embryonic melanophore migration, a function regulated by *kit* signaling. To test the interaction between *foxd3* and *kit* during melanogenesis, we reduced *foxd3* protein levels using translation blocking *foxd3* MO in *kit*^{w34} embryos. Following injection of *foxd3* MO at 1–2 cell stage, uninjected (control) and injected (foxd3MO) embryos were grown to 2dpf and images were taken. At 2dpf, *kit*^{w34} mutant melanophores are largely absent from the lateral and ventral stripes (compare AB (wildtype) to *kit*^{w34} in Fig. 2A and 2B). In *kit*^{w34}/*foxd3* morphants (Fig. 2C), more melanophores are present in the ventral stripe at 2dpf, as compared to controls (Fig. 2B, black arrow). Additional areas (near the otic vesicle, for example, red asterisks) appear to have more melanophores than uninjected controls.

To examine the temporal requirement for *kit* and *foxd3* in regulating melanophore numbers, control and *foxd3* MO injected AB (wildtype) and *kit*^{w34} larvae were collected at 2, 4 and 6 dpf and total melanophores were counted (Fig. 2D). At 2 dpf, the number of melanophores is similar under all conditions, despite the differences in distribution noted above. While melanophores continue to be added to wildtype animals over the next four days, melanophores are lost in *kit*^{w34}mutants, consistent with previous reports (Parichy et al.,

1999). This loss is significantly reduced in *kit*^{w34} mutants injected with *foxd3* MO as compared to uninjected controls. Uninjected and MO injected wildtype larvae have similar numbers of melanophores throughout this time course. Although *foxd3* MO injection strongly reduces *foxd3* protein production (Lister et al., 2006), it is conceivable that *kit foxd3* morphants retain some *foxd3* activity or MO efficacy is reduced at the times phenotypes are observed. To better characterize the importance of Foxd3 protein levels on melanophore development, we compared cell numbers in larvae mutant for both *kit* and *foxd3*. Consistent with our MO experiments, *kit*$^{w34/w34}$*;foxd3*$^{zdf10/zdf10}$ zebrafish show significant rescue in total melanophore numbers at 4dpf, as compared to *kit*$^{w34/w34}$ and *kit*$^{w34/w34}$*; foxd3*$^{zdf10/+}$ siblings (Table I). This data further supports a role for *foxd3* in the regulation of melanophore numbers in zebrafish.

foxd3 loss-of-function rescues melanophore localization in *kit*^{w34} mutants

Along with changes in melanophore numbers, we examined melanophore localization in *kit*^{w34} mutants injected with *foxd3* MO. During quantification of total melanophores, cell location at 2, 4, 6 and 8dpf was noted for each condition: melanophores localized to the lateral and ventral stripes were designated as migrated or peripheral melanophores, and those localized to the head and dorsal trunk areas were designated unmigrated or dorsal melanophores. Dorsal trunk melanophores, initially present in higher numbers in controls, persist longer in animals injected with *foxd3* MO, resulting in a significant increase at 8dpf (Fig. 3A). Peripherally localized melanophores are significantly increased with *foxd3* loss-of-function as indicated by quantification (Fig. 3B). Taken together, these data suggest that along with influencing cell number, *foxd3* activity inhibits embryonic melanophore migration in *kit* zebrafish mutants.

Melanophore specification is unaltered in *kit*^{w34}/*foxd3* morphants

To test whether *foxd3* interacts with *kit* signaling to regulate melanophore specification from neural crest cells, *kit*^{w34} embryos were injected with *foxd3* MO and examined by in situ hybridization. Melanophore precursors were visualized using RNA antisense probes for the *mitfa* and *dopachrome tautomerase* (*dct*) genes, which are markers for melanophore specification and differentiation, respectively (Lister et al., 1999; Kelsh et al., 2000). At 21 hours post fertilization (hpf), *mitfa* is detected in several distinct patches caudal to the eye and in the anterior trunk. Comparison of *mitfa* expression in uninjected and MO injected *kit*^{w34} embryos indicates similar levels of transcript at this stage (Figure 4A and 4B). Later at 25 hpf, some differentiating melanoblasts marked by *dct* expression are migrating ventrally from the dorsal trunk (black arrows, Fig 4C), while some cells remain in clumps caudal to the otic vesicle (red arrow, Fig 4C). Although a slight decrease in dorsal stripe melanoblasts is apparent with *foxd3* loss-of-function (compare Fig. 4C and 4D, black arrows), *kit*^{w34} embryos injected with *foxd3* MO show similar melanophore characteristics and *dct* expression levels to uninjected controls at 25 hpf. Thus, *foxd3* MO injection does not appear to affect melanoblast specification or differentiation from neural crest in *kit*^{w34} mutants, consistent with previous results in wildtype embryos (Lister et al., 2006).

To confirm that *kit* loss-of-function primarily affects melanophore survival and not other neural crest derivatives, we analyzed expression patterns of *foxd3* and *sox10* in *kit*^{w34} and wildtype embryos. *sox10* is expressed by all neural crest cells and critical for their differentiation into pigment and glia cells (Dutton et al., 2001). *foxd3*, expressed primarily by neural crest derived glia at 25hpf (Kelsh et al., 2000), is not affected by *kit* loss-of-function, as compared to wildtype (AB) embryos (Fig. 4E and 4F). Consistently, *sox10* expression in trunk premigratory neural crest cells (Fig. 4G and 4H, white arrows) is also largely unaffected by *kit* loss-of-function. There is some reduction in dorsal and peripheral *sox10* expression, consistent with the decrease in melanoblast numbers and migration

observed in *kit*^{w34} mutants. Taken together, these data suggest that *kit* and *foxd3* do not interact to increase the number of neural crest cells that give rise to melanoblasts. Furthermore, *foxd3* expression is not regulated by *kit* function, suggesting that the observed genetic interaction between these two genes is by some other mechanism.

foxd3 loss-of-function rescues melanophore morphology and survival in distinct *kit* alleles

Following specification, melanophores begin to process migratory and survival signals. As previously described, melanophore migration and survival both depend on *kit* function (Parichy et al., 1999). We hypothesized that *foxd3* inhibits melanophore survival, and thus *foxd3* loss-of-function rescues some *kit*-dependent melanophores from death. An alternative explanation is that increases in melanophores result from other neural crest cells switching fates to the melanophore lineage when the function of both genes is inhibited. To distinguish between these two possibilities, we utilized previously characterized *kit* zebrafish mutants, *kit*^{j1e60} and *kit*^{j1e78} (Rawls and Johnson, 2003). Unlike the *kit*^{b5} and *kit*^{w34} mutations, the *kit*^{j1e60} and *kit*^{j1e78} mutations have partial, distinct defects in *kit* signaling: 1) the *kit*^{j1e60} allele encodes a single amino acid substitution in the second IgG repeat of the extracellular domain (C146R), a portion of the receptor thought to participate in ligand binding (Blechman et al., 1993; Lev et al., 1993; Rawls and Johnson, 2003). This mutation renders melanophores deficient in migration to peripheral locations. However, the number of *kit*^{j1e60} melanophores remains fairly constant throughout embryonic development. 2) The *kit*^{j1e78} allele encodes a single amino acid substitution in the intracellular domain of the receptor (A779T). *kit*^{j1e78} melanophores are deficient in processing survival signals, yet migration patterns are similar to that of wildtype fish (Rawls and Johnson, 2003). We reasoned that if blocking *foxd3* function was promoting survival, then we should see increases in melanophores after *foxd3* MO injection in *kit*^{j1e78} but not *kit*^{j1e60} mutants. If additional melanophores were coming from another source, then we predicted to see increases in both mutants.

We injected *kit*^{j1e60} melanophore migration mutants with *foxd3* MO and examined their melanophores. Melanophore morphology (Fig. 5A – 5D) in *kit*^{j1e60} *foxd3* morphants is similar to uninjected controls. Furthermore, we do not detect significant increases in total melanophores at any time point examined (Fig. 5E). To confirm that our *foxd3* MO worked as expected in these experiments, we tallied trunk and tail iridophores at 4 dpf, which are known to be reduced by *foxd3* loss-of-function (Lister et al., 2006; Stewart et al., 2006). Indeed, iridophores are reduced in *kit*^{j1e60}/*foxd3* morphants (18 ± 14 iridophores) as compared to uninjected controls (52 ± 3 iridophores; Fig. 5A and 5B, black arrows). Consistent with results in *kit*^{w34} embryos, *foxd3* loss-of-function in *kit*^{j1e60} mutants increases melanophore localization to areas away from sites of origin (compare 5C and 5D, red arrows). Although the total number of melanophores does not increase in *kit*^{j1e60} mutants after *foxd3* MO injection, the extent of their migration over the head is restored closer to wildtype. These results further suggest that *foxd3* and *kit* play opposing roles in regulating melanophore migration.

We next examined the effects of *foxd3* loss-of-function in *kit*^{j1e78} melanophore survival mutants. We observe rounded, small melanophores, a phenotype indicative of apoptosis (Parichy et al., 1999), as early as 5dpf in the dorsal anterior trunk in control animals (Fig. 6A), and considerable changes in melanophore morphology with *foxd3* MO injection. *kit*^{j1e78}/*foxd3* morphants have flattened melanophores, a phenotype closer to that observed in wildtype larvae (Fig. 6A–C). Additionally, areas lacking melanophores in 5 dpf *kit*^{j1e78} embryos, presumably due to cell death, are partially rescued after MO injection (compare Fig. 6D and 6E). Quantification of melanophores at 2, 4 and 6 dpf confirms a significant increase in melanophores beginning at 4dpf (Fig. 6G). Iridophore counts confirm *foxd3* MO

function (average control and morphant iridophores ± standard deviation is 35 ± 12 and 4 ± 3, respectively).

To directly test the role of *foxd3* in melanophore survival, *kit*^{w34} larvae were injected with *foxd3* MO and examined by TUNEL assay at 3, 4 and 5dpf. Since previous studies suggest the number of TUNEL positive cells begins to increase in *kit*^{b5} mutants at 3dpf and peaks at 5.6dpf (Parichy et al., 1999), we decided to examine these same time points in our *kit*^{w34} mutants. TUNEL positive melanophore carcasses are most abundant in control 3dpf *kit*^{w34} larvae and often observed in apparent clusters (Fig. 7A–C, arrowheads). A significant decrease in melanophore carcasses is detected at 3dpf in *kit*^{w34} *foxd3* morphants (Fig. 7C). Although the number of TUNEL positive carcasses in *kit*^{w34} larvae is highest at 3dpf, they are visible at all time points examined. Taken together, these data suggest that *foxd3* regulates melanophore number by antagonizing *kit*-dependent melanophore survival, between 2 and 3dpf.

Ectopic expression of *foxd3* leads to precocious melanoblast death in *kit*^{w34} mutants

Given that *foxd3* loss-of-function rescues melanophore survival in *kit*^{w34} zebrafish larvae, we predicted that its ectopic expression would induce melanophore death. To test this possibility, we expressed myc epitope tagged-*foxd3* under the control of a heatshock promoter (*hs:mycfoxd3*), to bypass the early requirement for *foxd3* during zebrafish gastrulation and mesoderm induction (Steiner et al., 2006). Following injection of *hs:mycfoxd3* into embryos resulting from a *kit*^{w34}/+ intercross, *kit*^{w34} and wildtype embryos were grown to 19hpf and heat shocked at 37°C for 1 hour. We looked for *foxd3* expressing cells that showed fragmentation and blebbing, indicators of apoptosis, at 28hpf, when *kit* signaling is not yet required for melanophore survival (Rawls and Johnson, 2003). *kit* mutant animals were identified by their characteristic migration pattern. *kit*^{w34} larvae transgenic for green fluorescent protein (gfp) driven by a previously characterized 836bp portion of the *mitfa* promoter (*Tg(mitfa:gfp)*^{w47} Lister *et al*., in preparation; Dorsky et al., 2000) were used for identification of melanoblasts. Once embryos with fragmenting cells were identified, confocal images were taken of each embryo and the number of gfp/*foxd3*+ cells was counted (Table 2). Although we observe gfp/*foxd3*+ cells with wildtype morphology in both wildtype and *kit*^{w34} embryos (representative examples shown in Fig. 8A, 8G–H, white arrows), we observe fragmenting gfp/*foxd3*+ cells only in *kit*^{w34} embryos (representative examples shown in Fig. 8A–F, 8I–K, white asterisk and arrowheads; see Table 2 for quantification and statistical analysis). These results demonstrate that *foxd3* expression promotes melanophore death in the absence of *kit* function.

DISCUSSION

Our results indicate a genetic interaction between *foxd3* and *kit* during embryonic melanophore development that functions to regulate melanophore migration and survival. *foxd3* loss-of-function increases the number of melanophores in peripheral locations and significantly increases the total number of melanophores in three distinct *kit* melanophore survival alleles: *kit*^{w34} (null), *kit*^{b5} (null; data not shown) and *kitj1e78* (melanophore survival mutant). In situ hybridization analysis of *kit*^{w34} melanophore precursors after *foxd3* MO injection suggests that melanophore specification is unaltered, although additional cell counts at early stages might more definitively resolve this issue. Quantification of total melanophores in *kitj1e60* (melanophore migration) mutants following *foxd3* MO injection, suggests that *foxd3* dependent derivatives are not being redirected from other neural crest lineages to the melanophore lineage. Total melanophore numbers are similar between uninjected control and MO injected larvae at 2dpf in *kit*^{w34} and *kit j1e78 foxd3* MO experiments, providing additional support for *foxd3* function at a later stage of *kit*-dependent embryonic melanophore development. Last, examination of indicators of apoptosis (TUNEL

and cell fragmentation) in *foxd3* loss and gain of function conditions, respectively, suggest that *foxd3* promotes melanophore death, probably between 2 and 3dpf. These data suggest that *foxd3* modulates *kit* migration and survival function during zebrafish melanogenesis.

Function of *foxd3* and *kit* interaction during melanophore development

Our data suggests a genetic interaction between *kit* and *foxd3* activity, that initially regulates migration (prior to 2dpf), then later, melanophore survival (post 2dpf). *foxd3* loss-of-function significantly decreases apoptosis in kit^{w34} melanophores at 3dpf, a process known to be regulated by *kit* signaling. Overexpression of *foxd3* via heatshock at 19hpf, a time when *kit* is not required for promoting melanophore survival (Rawls and Johnson, 2003), induced precocious cell death (as indicated by cell fragmentation) in *kit* null larvae, only. These results suggest that *foxd3* and *kit* act antagonistically in the regulation of cell survival. Regulation of migration is somewhat more complicated. Loss of either *kit* or *foxd3* function results in a reduction of ventrally migrating melanophores, which might suggest that the wildtype function both promote migration, while the combined loss of both somewhat restores migration. However, the combined loss-of-function reveals antagonistic interactions. Future studies using time-lapse analysis may help resolve whether alterations in migration are due to changes in motility.

There are several mechanisms that may explain the genetic interaction observed between *kit* and *foxd3*. The two genes might function in the same pathway. *foxd3* could act upstream of *kit* signaling to regulate melanophore survival. This mechanism supposes that some *kit* activity remains in mutants, and this activity is enhanced by loss of *foxd3*. However, both *kit* null alleles show enhanced melanophore survival after *foxd3* loss of function. Since the kit^{w34} mutant is a deletion resulting in a frameshift, we think it unlikely that it has any residual activity. Alternatively, *foxd3* might act downstream of *kit*, with *kit* signaling functioning to downregulate *foxd3* activity. In the absence of *kit* function, an increase in *foxd3* activity would disrupt melanophore migration and survival; and conversely loss of *foxd3* activity would therefore partially rescue the *kit* mutant phenotype. Consistently, *kit* signaling has been found to deactivate other members of the forkhead transcription factor family, FoxO1 and FoxO3, in multipotent progenitor cell lines, by controlling trafficking of these forkhead proteins out of the nucleus (Engstrom et al., 2003).

It is also conceivable that *kit* regulates another factor that is parallel or downstream to *foxd3* activity that functions in melanophore migration and/or survival, such as *mitfa*. As one function of mouse Mitf is to transactivate *bcl-2*, which in turn would inhibit cell death (McGill et al., 2002), the balance of Mitf activation and repression by *kit* and *foxd3* might explain their epistatic interaction. Activation of *kit* signaling results in increased Mitf transcriptional activity (Hemesath et al., 1998). Recent studies demonstrate that *foxd3* directly represses *mitfa* activity (Curran et al., submitted). Consistently, histone deacetylase 1 dependent reduction of *foxd3* expression is necessary to increase *mitfa* expression and subsequent specification of melanoblasts from neural crest cells (Ignatius et al., 2008). We presume that activity of *mitfa* is not a limiting factor for cell survival in wildtype animals, since *foxd3* loss-of-function (resulting in increased *mitfa* activity) has no effect on melanophore numbers. We hypothesize that *mitfa* activity becomes limiting after its reduction with *kit* loss-of-function, and melanophore survival becomes sensitive to additional changes in *mitfa* activity resulting from manipulation of *foxd3*. Further experiments on the roles of zebrafish *foxd3* on *mitfa* expression and the temporal requirements for these distinct activities are needed to address this model.

kit signaling, *foxd3* and disease

Activating mutations in the *kit* receptor have been correlated with several types of cancer, including gastrointestinal stromal tumors (Hirota et al., 1998) and melanoma (Lefevre et al., 2004). Loss-of-function in mice has been associated with sterility and anemia, as *kit* plays a critical role in promoting the survival of primordial germ cells and hematopoetic precursor cells in mammals. One disorder linked to defects in both *kit* and *foxd3* expression is the melanocyte specific disorder, Vitiligo, which results from a gradual loss of pigment cells and is characterized by light patches of skin and hair (reviewed in Imokawa, 2004; Goding, 2007). The exact mechanisms underlying the progression of Vitiligo are not entirely understood, but one mechanism being explored involves the loss of expression and/or activity of key melanocyte survival genes, including *kit* and its downstream targets, Mitf and *bcl-2*. Conversely, the link between Vitiligo and *foxd3* involves overexpression. An uncommon variant sequence in the *foxd3* promoter, - 639G>T, was linked to patients with Vitiligo (Alkhateeb et al., 2005). Additional characterization of the variant promoter in luciferase assays suggests it has higher transcriptional activity than the wildtype promoter in cells expressing *foxd3* endogenously. The authors suggest a model where melanoblast precursors containing the variant promoter sequence, may have enhanced *foxd3* expression, leading to alterations in melanocyte development (Alkhateeb et al., 2005). At what stage of Vitiligo progression *foxd3* may exert its effect is unclear, however, it is plausible that the relationship between *kit* and *foxd3* plays a role in promoting normal melanocyte number, function and homeostasis.

EXPERIMENTAL PROCEDURES

Fish rearing and crosses

Wildtype fish were of the AB (ZDB-GENO-960809-7) strain. Adult zebrafish were maintained on a 14-h/10-h light/dark cycle at 28.5°C. Embryos were acquired from natural crosses, grown at 28.5°C in embryo media until analysis. Embryos were staged according to characterized morphological criteria (Kimmel et al., 1995). The following alleles were used: $kita^{b5}$, (Parichy et al., 1999); $kita^{j1e60}$, $kita^{j1e78}$ (Rawls and Johnson, 2003); $foxd3^{zdf10}$, (Stewart et al., 2006); $Tg(mitfa:gfp)^{w47}$, (Lister et al., in prep).

Isolation, characterization and sequencing of kit^{w34}

For mutagenesis, adult AB males were treated with *N*-ethyl *N*-nitrosourea according to published methods (Solnica-Krezel et al., 1994) and outcrossed to wild-type females. These F1 progeny were intercrossed and the kit^{w34} mutation was identified by intercrossing adults from one of the resulting F2 families. Complementation analysis was done by crossing homozygous kit^{w34} females with homozygous kit^{b5} males. Live embryos were examined for rescue of melanophore migration and survival.

For sequencing the kit^{w34} allele, total RNA was isolated from 24hpf AB and kit^{w34} embryos using Trizol (Invitrogen, Carlsbad CA) according to manufacturer's recommendations, followed by cDNA preparation (Superscript First Strand Kit; Invitrogen, Carlsbad CA). PCR primers (sequences available on request), designed to amplify 6 overlapping regions of *kita* cDNA, and subsequent gel analysis revealed a difference in migration for one specific PCR product, as compared to wildtype. The variant amplicon was sequenced, revealing a large gap in *kita* cDNA. PCR primers designed to amplify area adjacent to the gap were used to amplify kit^{w34} genomic DNA. Subsequent gel analysis confirmed kit^{w34} embryos were lacking exon 10 (along with some adjacent intron DNA), resulting in a frameshift and early stop codon.

MO injection and live imaging

Embryos obtained from natural matings were injected at the 1–2 cell stage with *foxd3* MO oligonucleotide designed to bind the 5' untranslated region of *foxd3* message (Lister et al., 2006). Volumes and concentrations ranged from 0.5–1nL per embryo of 1–2mg/mL working stocks. A 10mg/mL MO stock was diluted in 1X Danieu Buffer (58 mM NaCl, 0.7mM KCl, 0.4 mM MgSO4, 0.6 mM Ca(NO3)2, 5.0 mM HEPES pH 7.6) to generate working stocks.

For imaging, live fish were anesthetized in MESAB (MS-222; Sigma, St Louis, MO) and immobilized in 3% methyl cellulose. Fish were visualized using Nikon SMZ1500 dissecting or Zeiss Axioplan 2 microscopes. Brightfield images were taken using a Spot Camera and Spot advanced software program. Images were processed for color balance and brightness/ contrast using Adobe Photoshop Elements 4.0.

Melanophore and iridophore counts

Fish were grown to the appropriate stage at 28.5°C, then soaked in 5mg/mL epinephrine for 5–10 minutes (in embryo media) to aggregate melanosomes around the cell body and improve visibility of individual cells. Larvae were fixed in 4% paraformaldehyde at room temperature for 1–2h or 14–18h at 4°C. Melanophores and iridophores were quantified using dissecting microscopes and intact fixed fish (not images). To assist with iridophore visualization and counting, epi-illumination from a fiber optic light source was used. Tail and trunk iridophores were quantified. "Total" melanophores include cells found in the dorsal and lateral stripes, as well as ventral stripe cells found posterior to the cloaca. In kit^{w34} *foxd3* MO experiments, the complete ventral stripe was counted. Statistical tests were performed using Prism 5.0 (Graphpad Software, San Diego, CA)

In situ hybridization

Embryos were fixed in 4% paraformaldehyde (in phosphate buffered saline, pH 7.2) and processed using standard protocols. Digoxygenin-labeled probes for *mitfa* (Lister et al., 1999), *dopachrome tautamerase* (Kelsh et al., 2000), *sox10* (ZDB-GENE-011207-1; Dutton et al., 2001), *foxd3* (ZDB-GENE-980526-143; Odenthal and Nusslein-Volhard, 1998) and *kita* genes (Parichy et al., 1999) have been previously described. Fluorescent in situ hybridization was done using a protocol developed in Scott Holley's laboratory (Julich et al., 2005).

Melanophore TUNEL analysis

TUNEL analysis was done using In Situ Cell Death Detection Kits (Roche, Indianapolis, IN) using the below protocol adapted from C. Moens, R. Kelsh and S. Holley laboratory protocols. Fish were fixed in 4% paraformaldehyde for 1–2 hours at RT or 12–16 hours at 4°C. Larvae were dehydrated, then rehydrated in 25:75, 50:50, 75:25 MEOH/Tris buffered saline (1M Tris, pH 7.5, 1.5M NaCl) containing 2% Triton-X 100 and 5% Tween-20 (TBSTT), 5–10 minutes each. Larvae were incubated in Proteinase K (1ug/ml) diluted in TBSTT for 30 minutes at RT, with continuous rocking. Proteinase K activity was quenched in 2mg/ml glycine, larvae were fixed for 20 minutes in 4% paraformaldehyde and washed in TBSTT. Larvae were washed in Roche TUNEL dilution buffer, incubated in TUNEL enzyme/label mix (Roche In Situ Cell Death Detection kit) for 1 hour on ice, followed by 1 hour incubation at 37°C, protected from light. Larvae were washed in TBSTT, blocked in 150mM maleic acid, 100mM NaCl, (pH 7.5) plus 2% Western Blocking Reagent (Roche, Indianapolis, IN) and incubated in anti-fluor- POD antibody (Roche, Indiananapolis, IN; 1:1000 dilution) for 12–16 hours at 4°C. Next, larvae were washed in maleic acid/NaCl buffer and incubated in TSA plus fluorescein solution (Invitrogen, Carlsbad, CA) for 45–60 minutes. Larvae were dehydrated in MEOH/PBS series, incubated in 1% H2O2 in 100%

MEOH, followed by rehydration. Larvae were visualized and imaged using Nikon SMZ1500 dissecting or Zeiss Axioplan 2 microscopes.

Ectopic expression of *foxd3* and confocal imaging

Intercrossed *kit*^{w34}/+ fish, transgenic for mitfa:gfp (Tg(mitfa:gfp)^{w47}; Lister et al., in preparation), were injected with *foxd3* under the control of the zebrafish *hsp70* heatshock promoter (Halloran et al., 2000) at the 1–2 cell stage. At approximately 19hpf, fish were transferred from 28°C to 37°C for 1 hour, and returned to 28°C until fixation at 28hpf. Following fixation, fish were blocked in antibody block (1xPBS, 0.2% Triton X-100, 2mg/ml BSA, 1%DMSO, 0.02% Na Azide) supplemented with 5% goat serum for at least 1 hour. Fish were stained overnight in mouse anti-Myc (Cell Signaling Technology, Danvers MA) and rabbit anti-GFP (Invitrogen/Molecular Probes, Carlsbad CA) antibodies at 4°C. Fish were washed in PBT (PBS + 0.1% Triton X-100) then stained overnight in anti-mouse Alexa 568 and anti-rabbit Alexa-488 secondary antibodies (Invitrogen/Molecular Probes, Carlsbad CA). Fish were washed in PBT, deyolked and mounted for confocal imaging, using a Zeiss LSM Pascal confocal microscope. Images were processed for color balance and contrast/brightness using Adobe Photoshop Elements 4.0.

Acknowledgments

The authors would like to thank Dave White and all current and previous members of the UW Fish Facility for excellent fish care. David Parichy, James Lister and Kevin Curran for critical evaluation of the manuscript. Keith Hultman and Steve Johnson for providing *kit*^{j1e78} and *kitj1e60* zebrafish mutants. John Kanki and A. Thomas Look for providing *foxd3*^{zdf10} /*foxd3* zebrafish mutants. This work was supported by a NIH National Research Service Award to C.D.C and a NIH RO1 grant to D.W.R.

Grant sponsor: National Institutes of Health

Grant number: 1F32 HD047108-01 to CDC, 1R01-NS45246 to DWR

REFERENCES

Alkhateeb A, Fain PR, Spritz RA. Candidate functional promoter variant in the FOXD3 melanoblast developmental regulator gene in autosomal dominant vitiligo. Journal of Investigative Dermatology. 2005; 125:388–391. [PubMed: 16098053]

Bernex F, De Sepulveda P, Kress C, Elbaz C, Delouis C, Panthier JJ. Spatial and temporal patterns of c-kit-expressing cells in WlacZ/+ and WlacZ/WlacZ mouse embryos. Development. 1996; 122:3023–3033. [PubMed: 8898216]

Blechman JM, Lev S, Brizzi MF, Leitner O, Pegoraro L, Givol D, Yarden Y. Soluble c-kit proteins and antireceptor monoclonal antibodies confine the binding site of the stem cell factor. Journal of Biological Chemistry. 1993; 268:4399–4406. [PubMed: 7680037]

Cooper CD, Raible DW. Mechanisms for reaching the differentiated state: Insights from neural crest derived melanocytes. Sem Cell Dev Biol 2008. 2008 Sep 30. [Epub ahead of print].

Copeland NG, Gilbert DJ, Cho BC, Donovan PJ, Jenkins NA, Cosman D, Anderson D, Lyman SD, Williams DE. Mast cell growth factor maps near the steel locus on mouse chromosome 10 and is deleted in a number of steel alleles. Cell. 1990; 63:175–183. [PubMed: 1698554]

Cornell RA, Yemm E, Bonde G, Li W, d'Alencon C, Wegman L, Eisen J, Zahs A. Touchtone promotes survival of embryonic melanophores in zebrafish. Mech Dev. 2004; 121:1365–1376. [PubMed: 15454266]

Dorsky RI, Moon RT, Raible DW. Control of neural crest cell fate by the Wnt signalling pathway. Nature. 1998; 396:370–373. [PubMed: 9845073]

Dorsky RI, Raible DW, Moon RT. Direct regulation of nacre, a zebrafish MITF homolog required for pigment cell formation, by the Wnt pathway. Genes Dev. 2000; 14:158–162. [PubMed: 10652270]

Dunn KJ, Brady M, Ochsenbauer-Jambor C, Snyder S, Incao A, Pavan WJ. WNT1 and WNT3a promote expansion of melanocytes through distinct modes of action. Pigment Cell Res. 2005; 18:167–180. [PubMed: 15892713]

Dutton KA, Pauliny A, Lopes SS, Elworthy S, Carney TJ, Rauch J, Geisler R, Haffter P, Kelsh RN. Zebrafish colourless encodes sox10 and specifies non-ectomesenchymal neural crest fates. Development. 2001; 128:4113–4125. [PubMed: 11684650]

Engstrom M, Karlsson R, Jonsson JI. Inactivation of the forkhead transcription factor FoxO3 is essential for PKB-mediated survival of hematopoietic progenitor cells by kit ligand. Experimental Hematology. 2003; 31:316–323. [PubMed: 12691919]

Geissler EN, Ryan MA, Housman DE. The dominant-white spotting (W) locus of the mouse encodes the c-kit proto-oncogene. Cell. 1988; 55:185–192. [PubMed: 2458842]

Goding CR. Melanocytes: The new Black. The International Journal of Biochemistry and Cell Biology. 2007; 39:275–279.

Hirota S, Isozaki K, Moriyama Y, Hashimoto K, Nishida T, Ishiguro S, Kawano K, Hanada M, Kurata A, Takeda M, Muhammad Tunio G, Matsuzawa Y, Kanakura Y, Shinomura Y, Kitamura Y. Gain-of-function mutations of c-kit in human gastrointestinal stromal tumors. Science. 1998; 279:577–580. [PubMed: 9438854]

Hodgkinson CA, Moore KJ, Nakayama A, Steingrimsson E, Copeland NG, Jenkins NA, Arnheiter H. Mutations at the mouse microphthalmia locus are associated with defects in a gene encoding a novel basic-helix-loop-helix-zipper protein. Cell. 1993; 74:395–404. [PubMed: 8343963]

Ignatius MS, Moose HE, El-Hodiri HM, Henion PD. colgate/hdac1 Repression of foxd3 expression is required to permit mitfa-dependent melanogenesis. Dev Biol. 2008; 313:568–583. [PubMed: 18068699]

Imokawa G. Autocrine and paracrine regulation of melanocytes in human skin and in pigmentary disorders. Pigment Cell Research. 2004; 17:96–110. [PubMed: 15016298]

Johnson SL, Africa D, Walker C, Weston JA. Genetic control of adult pigment stripe development in zebrafish. Developmental Biology. 1995; 167:27–33. [PubMed: 7851648]

Julich D, Hwee Lim C, Round J, Nicolaije C, Schroeder J, Davies A, Geisler R, Lewis J, Jiang YJ, Holley SA. beamter/deltaC and the role of Notch ligands in the zebrafish somite segmentation, hindbrain neurogenesis and hypochord differentiation. Dev Biol. 2005; 286:391–404. [PubMed: 16125692]

Kelsh RN, Schmid B, Eisen JS. Genetic analysis of melanophore development in zebrafish embryos. Developmental Biology. 2000; 225:277–293. [PubMed: 10985850]

Kimmel CB, Ballard WW, Kimmel SR, Ullmann B, Schilling TF. Stages of embryonic development of the zebrafish. Developmental Dynamics. 1995; 203:253–310. [PubMed: 8589427]

Kos R, Reedy MV, Johnson RL, Erickson CA. The winged-helix transcription factor FoxD3 is important for establishing the neural crest lineage and repressing melanogenesis in avian embryos. Development. 2001; 128:1467–1479. [PubMed: 11262245]

Lefevre G, Glotin AL, Calipel A, Mouriaux F, Tran T, Kherrouche Z, Maurage CA, Auclair C, Mascarelli F. Roles of stem cell factor/c-Kit and effects of Glivec/STI571 in human uveal melanoma cell tumorigenesis. Journal of Biological Chemistry. 2004; 279:31769–31779. [PubMed: 15145934]

Lev S, Blechman J, Nishikawa S, Givol D, Yarden Y. Interspecies molecular chimeras of kit help define the binding site of the stem cell factor. Molecular & Cellular Biology. 1993; 13:2224–2234. [PubMed: 7681144]

Lister JA, Cooper C, Nguyen K, Modrell M, Grant K, Raible DW. Zebrafish Foxd3 is required for development of a subset of neural crest derivatives. Developmental Biology. 2006; 290:92–104. [PubMed: 16364284]

Lister JA, Robertson CP, Lepage T, Johnson SL, Raible DW. nacre encodes a zebrafish microphthalmia-related protein that regulates neural-crest-derived pigment cell fate. Development. 1999; 126:3757–3767. [PubMed: 10433906]

McGill GG, Horstmann M, Widlund HR, Du J, Motyckova G, Nishimura EK, Lin YL, Ramaswamy S, Avery W, Ding HF, Jordan SA, Jackson IJ, Korsmeyer SJ, Golub TR, Fisher DE. Bcl2 regulation

by the melanocyte master regulator Mitf modulates lineage survival and melanoma cell viability. Cell. 2002; 109:707–718. [PubMed: 12086670]

McNeill MS, Paulsen J, Bonde G, Burnight E, Hsu MY, Cornell RA. Cell death of melanophores in zebrafish trpm7 mutant embryos depends on melanin synthesis. J Invest Dermatol. 2007; 127:2020–2030. [PubMed: 17290233]

Mellgren EM, Johnson SL. kitb, a second zebrafish ortholog of mouse Kit. Development Genes & Evolution. 2005; 215:470–477. [PubMed: 16096802]

Montero-Balaguer M, Lang MR, Sachdev SW, Knappmeyer C, Stewart RA, De La Guardia A, Hatzopoulos AK, Knapik EW. The mother superior mutation ablates foxd3 activity in neural crest progenitor cells and depletes neural crest derivatives in zebrafish. Dev Dyn. 2006; 235:3199–3212. [PubMed: 17013879]

Opdecamp K, Nakayama A, Nguyen MT, Hodgkinson CA, Pavan WJ, Arnheiter H. Melanocyte development in vivo and in neural crest cell cultures: crucial dependence on the Mitf basic-helix-loop-helix-zipper transcription factor. Development. 1997; 124:2377–2386. [PubMed: 9199364]

Parichy DM, Rawls JF, Pratt SJ, Whitfield TT, Johnson SL. Zebrafish sparse corresponds to an orthologue of c-kit and is required for the morphogenesis of a subpopulation of melanocytes, but is not essential for hematopoiesis or primordial germ cell development. Development. 1999; 126:3425–3436. [PubMed: 10393121]

Parichy DM, Turner JM. Zebrafish puma mutant decouples pigment pattern and somatic metamorphosis. Dev Biol. 2003; 256:242–257. [PubMed: 12679100]

Rawls JF, Johnson SL. Temporal and molecular separation of the kit receptor tyrosine kinase's roles in zebrafish melanocyte migration and survival. Developmental Biology. 2003; 262:152–161. [PubMed: 14512025]

Sauka-Spengler T, Bronner-Fraser M. Development and evolution of the migratory neural crest: a gene regulatory perspective. Current Opinion in Genetics & Development. 2006; 16:360–366. [PubMed: 16793256]

Silver DL, Hou L, Somerville R, Young ME, Apte SS, Pavan WJ. The secreted metalloprotease ADAMTS20 is required for melanoblast survival. PLoS Genet. 2008; 4:e1000003. [PubMed: 18454205]

Solnica-Krezel L, Schier AF, Driever W. Efficient recovery of ENU-induced mutations from the zebrafish germline. Genetics. 1994; 136:1401–1420. [PubMed: 8013916]

Steiner AB, Engleka MJ, Lu Q, Piwarzyk EC, Yaklichkin S, Lefebvre JL, Walters JW, Pineda-Salgado L, Labosky PA, Kessler DS. FoxD3 regulation of Nodal in the Spemann organizer is essential for Xenopus dorsal mesoderm development. Development. 2006; 133:4827–4838. [PubMed: 17092955]

Stewart RA, Arduini BL, Berghmans S, George RE, Kanki JP, Henion PD, Look AT. Zebrafish foxd3 is selectively required for neural crest specification, migration and survival. Developmental Biology. 2006; 292:174–188. [PubMed: 16499899]

Takeda K, Yasumoto K, Takada R, Takada S, Watanabe K, Udono T, Saito H, Takahashi K, Shibahara S. Induction of melanocyte-specific microphthalmia-associated transcription factor by Wnt-3a. J Biol Chem. 2000; 275:14013–14016. [PubMed: 10747853]

Widlund HR, Horstmann MA, Price ER, Cui J, Lessnick SL, Wu M, He X, Fisher DE. Beta-catenin-induced melanoma growth requires the downstream target Microphthalmia-associated transcription factor. J Cell Biol. 2002; 158:1079–1087. [PubMed: 12235125]

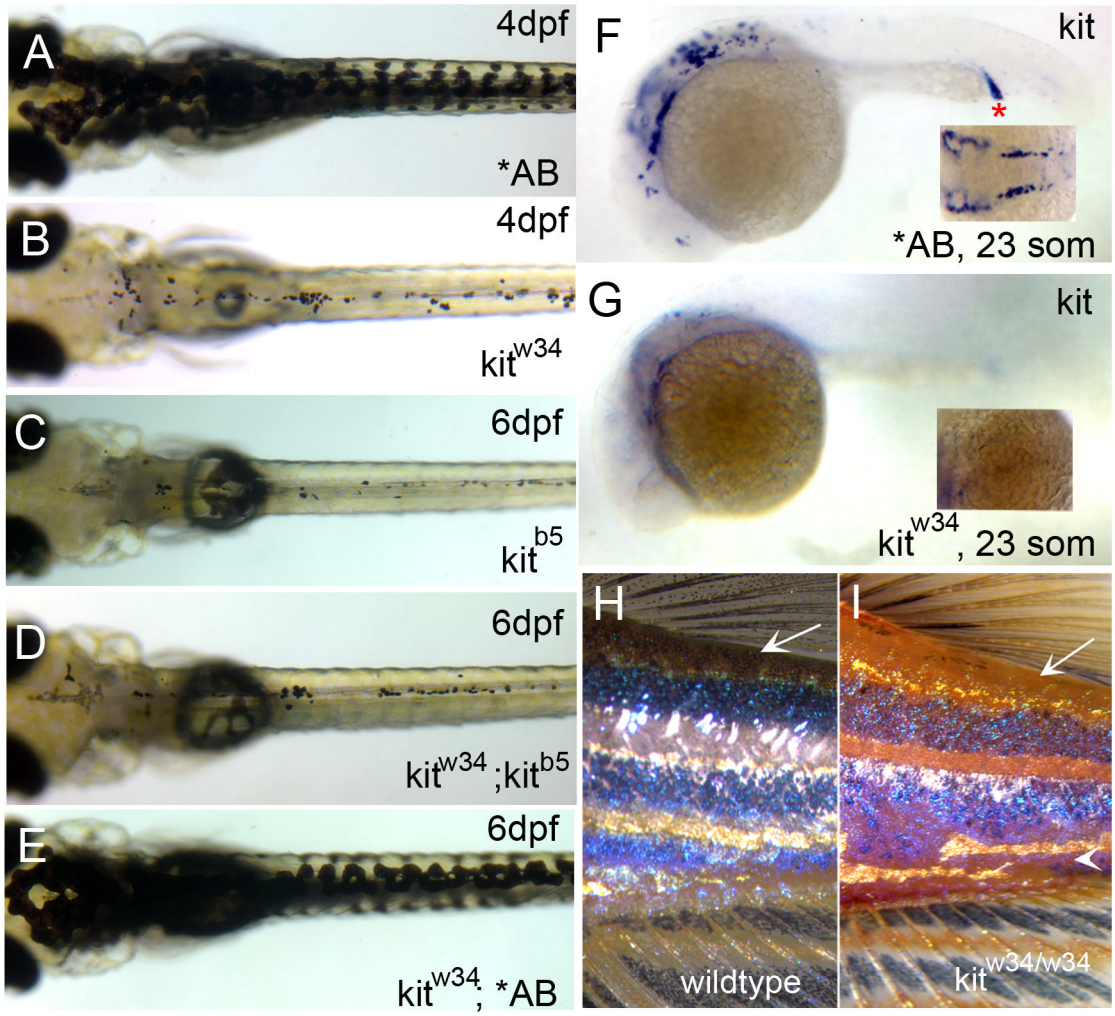

Fig. 1.

Characterization of *kit*^{w34} mutant larvae. (A) AB zebrafish at 4dpf, illustrating wildtype melanophore morphology and patterning. (B) *kit*^{w34} zebrafish at 4dpf, have small, rounded melanophores. Lateral and ventral stripe melanophores are largely missing by this stage. (C–E) *kit*^{w34}/*kit*^{b5} complementation analysis. (C) In *kit*^{b5}, 6dpf zebrafish, the majority of melanophores have died. (D) While progeny from a homozygous *kit*^{b5} and *kit*^{w34} cross show defects in melanophore morphology and survival, progeny from a *kit*^{w34} and AB cross are rescued and show wildtype melanophore patterning (E). (F, G) In situ analysis for *kit* mRNA during early melanogenesis. (F) Wildtype zebrafish express *kit* in the head, anterior trunk and intermediate cell mass (red asterisk) at 23 somites. (G) *kit*^{w34} embryos lack *kit* expression. H, I) *kit*^{w34} adults have a reduction in melanophores. (H) Wildtype pigment pattern showing three distinct dark stripes on the flank near the dorsal and caudal fins. (I) *kit*^{w34} adult showing reduced overall pigmentation, especially in dorsal areas (arrow) and throughout the dark stripes. The darks stripes are disorganized and the ventral stripe is lost with *kit* loss-of-function (arrowhead).

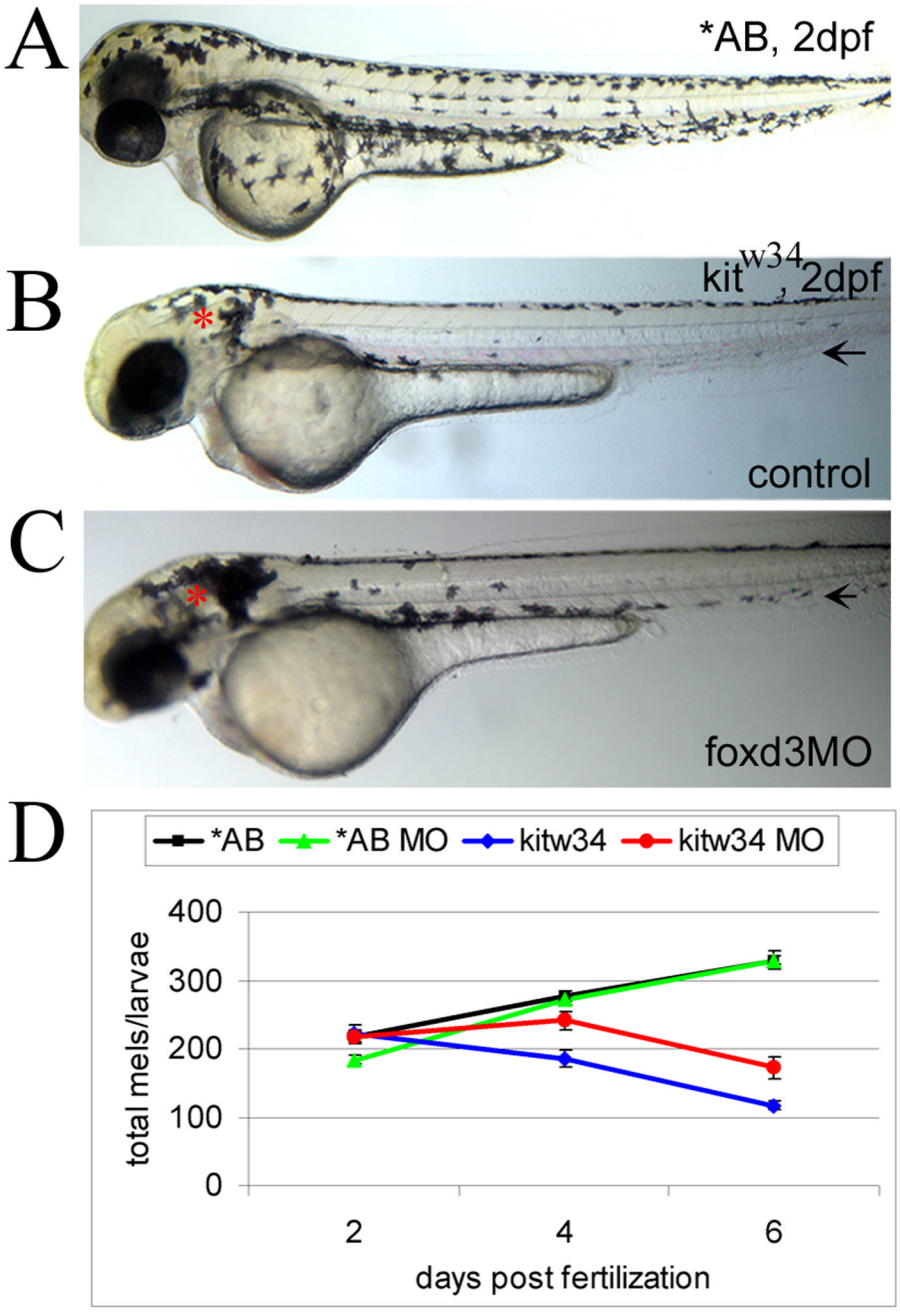

Fig. 2.

foxd3 loss-of-function reduces loss of melanophores in *kit*^{w34} zebrafish (A) In 2 dpf wildtype zebrafish (AB), melanophores have migrated extensively, anteriorly to the head and ventrally over the yolk. (B) In 2 dpf *kit*^{w34} zebrafish, melanophores are specified, but largely fail to migrate from sites of origin: the dorsal trunk and area caudal to the otic vesicle (red asterisk). (C) *kit*^{w34} zebrafish injected with *foxd3* MO have more melanophores, especially apparent near the otic vesicle (foxd3MO, red asterisk). Both the ventral and lateral stripes show an increase in melanophores (black arrows). (D) Line graph showing counts of total melanophores in 2, 4 and 6dpf AB or *kit*^{w34} larvae, either uninjected (control) or injected with *foxd3* MO. A significant change in the number of melanophores is observed

in *kit*^{w34} mutants after injection of *foxd3* MO (red) as compared to *kit*^{w34} uninjected controls (blue; $p<0.0001$ by 2-way ANOVA; 7–11 fish per time point), whereas AB *foxd3* morphants (green) show no significant difference as compared to uninjected AB controls (black; $p=0.49$ by 2-way ANOVA; 9–13 fish per time point).

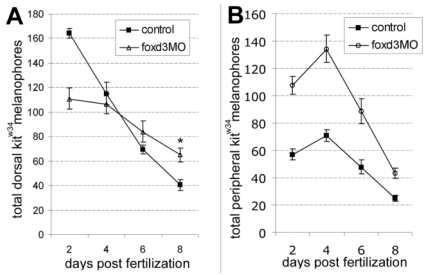

Fig. 3.

foxd3 loss-of-function alters the number of melanophores localized to the dorsal stripe and periphery. A) In the dorsal stripe, *kit*^{w34} control embryos (solid squares) lose melanophores quickly, showing a dramatic reduction by 8 dpf. Conversely, melanophores persist in *kit*^{w34} *foxd3* morphants at higher numbers (*, $p<0.05$ by Bonferroni posttest at 8 dpf). Note that dorsal melanophores are initially present at lower numbers in *kit*^{w34} animals injected with *foxd3* MO than in controls, but are present at higher numbers at 2 dpf in the periphery. B) The few melanophores detected in *kit*^{w34} lateral and ventral stripes (solid squares) at 2 dpf initially increase, and then steadily decline with each subsequent time point. Peripheral melanophores are detected at significantly higher numbers in 2 dpf in kit^{w34} *foxd3* morphants as compared to uninjected *kit*^{w34} controls at all time periods ($p<0.05$ a by Bonferroni posttest).

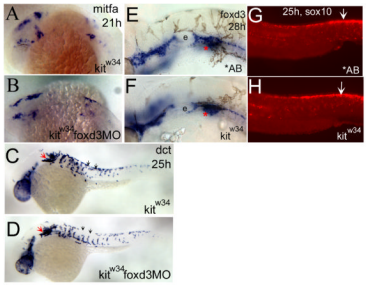

Fig. 4.

foxd3 loss-of-function does not affect the number of melanoblasts specified from *kit*^{w34} neural crest. A,B) *mitfa* expression is detected in the head and anterior trunk of *kit*^{w34} 21hpf embryos. This pattern is not dramatically altered in *kit*^{w34} *foxd3* morphants. C, D) In 25 hpf *kit*^{w34} embryos, *dopachrome tautomerase* (*dct*) positive cells are found caudal to the eye and ear (red arrow), and in streams migrating ventrally between somites from the dorsal trunk (black arrows). *kit*^{w34} *foxd3* morphants show some differences in migration (compare C and D, black arrows) but the overall number of cells appears similar. E, F) 28hpf AB and *kit*^{w34} embryos, processed by in situ hybridization for *foxd3* message. *foxd3* expression appears unchanged by *kit* loss-of-function. e; developing ear or otic vesicle G, H) 25hpf AB and *kit*^{w34} embryos, processed by fluorescent in situ hybridization for *sox10* message. *sox10* expression in premigratory neural crest cells is mostly unchanged (white arrows), although there is some reduction in peripheral expression, consistent with the reduction in melanoblast migration observed in *kit*^{w34} mutants.

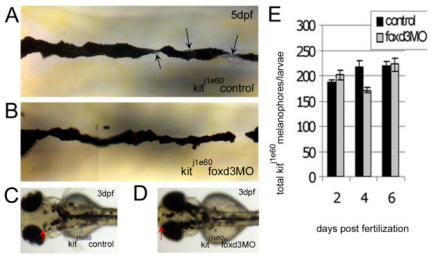

Fig. 5.

The increase in *kit* mutant melanophores with *foxd3* loss-of-function is not due to transfating of other *foxd3* dependent cell types. A-D) *kitj1e60* melanophore migration mutants were injected (or left uninjected; control) with *foxd3* MO (foxd3MO), imaged at 3 (C, D) and 5dpf (A, B) and fixed at 2, 4 and 6 dpf for melanophore quantification. A) Melanophores localized to the anterior dorsal trunk display relatively normal, non-apoptotic morphology. Black arrows indicate silver pigment cells, iridophores. B) In *kit*^{j1e60} *foxd3* morphants, *foxd3* dependent iridophores are gone indicating MO function (average control and morphant iridophores ± standard deviation at 4dpf are 52±3 and 18±14, respectively), yet melanophore morphology and number remain similar to uninjected controls. C) *kitj1e60* control melanophores do not localize to the anterior most portion of the head, indicating a migration defect. D) The presence of melanophores over the head is partially rescued with *foxd3* loss-of-function (red arrows indicate anterior extent of melanophores). E) *kitj1e60* melanophores are not significantly increased with *foxd3* loss-of-function at 2, 4 and 6 dpf ($p=0.31$ by 2-way ANOVA; 8–15 fish per time point).

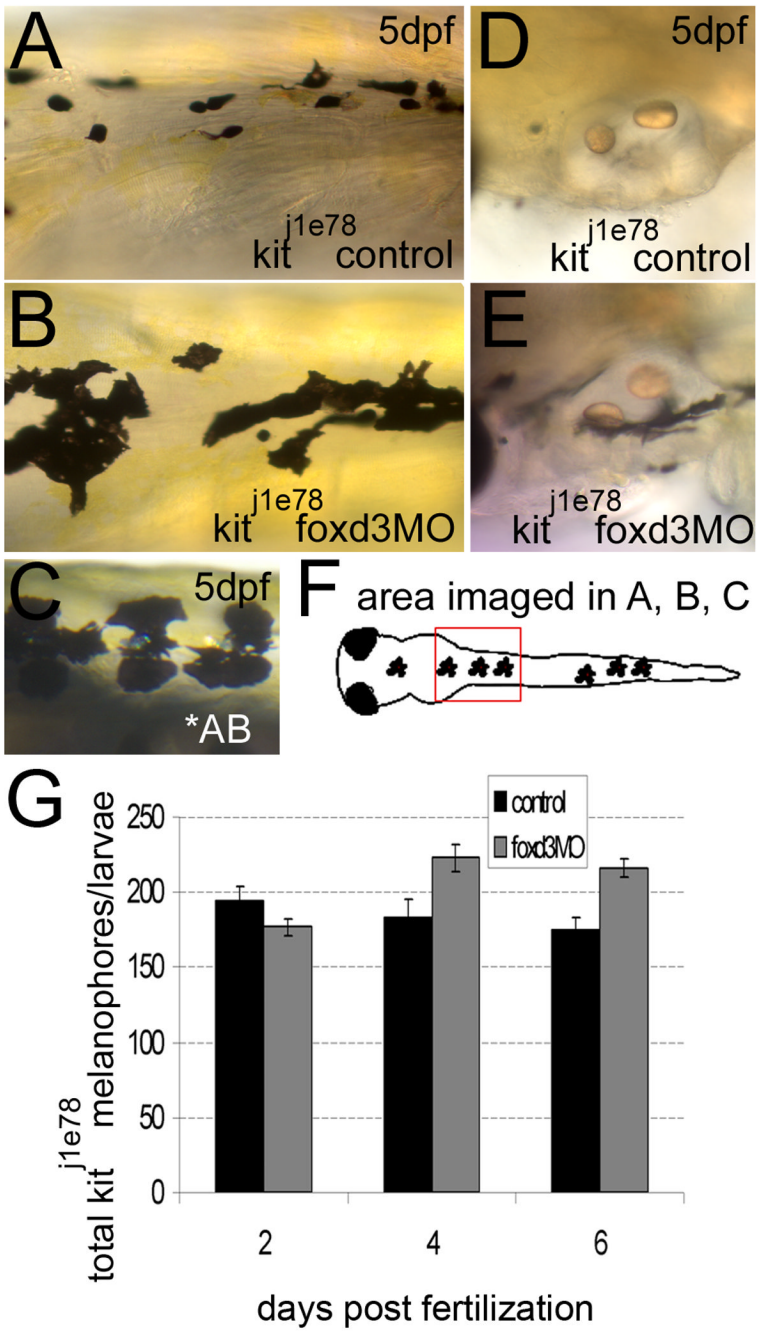

Fig. 6.

foxd3 loss-of-function improves the number and morphology of *kit j1e78* survival mutant melanophores. A, B, D, E) *kitj1e78* survival mutants were injected with *foxd3* MO (foxd3MO) or uninjected embryos were examined as controls. A) Control kit^{j1e78} melanophores are small and rounded, characteristic of apoptosing melanophores. B) loss of *foxd3* activity restores some wildtype morphology to kit^{j1e78} melanophores, and increases the number of melanophores (compare 6B to AB wildtype melanophores in 6C). D) kit^{j1e78} controls lack ventral stripe melanophores near the otic vesicle, which have apoptosed and been removed from the fish. E) kit^{j1e78} *foxd3* morphants show increases in melanophores at this location, suggesting increased survival. F) Cartoon illustrating the location of images

taken in A–C. G) Quantification at 2, 4 and 6 dpf of *kit*^{j1e78} and *kit*^{j1e78} *foxd3* morphant melanophores. There is a statistically significant increase in *kit*^{j1e78} animals after *foxd3* MO injection ($p<0.005$ by 2-way ANOVA; 10–19 fish per time point).

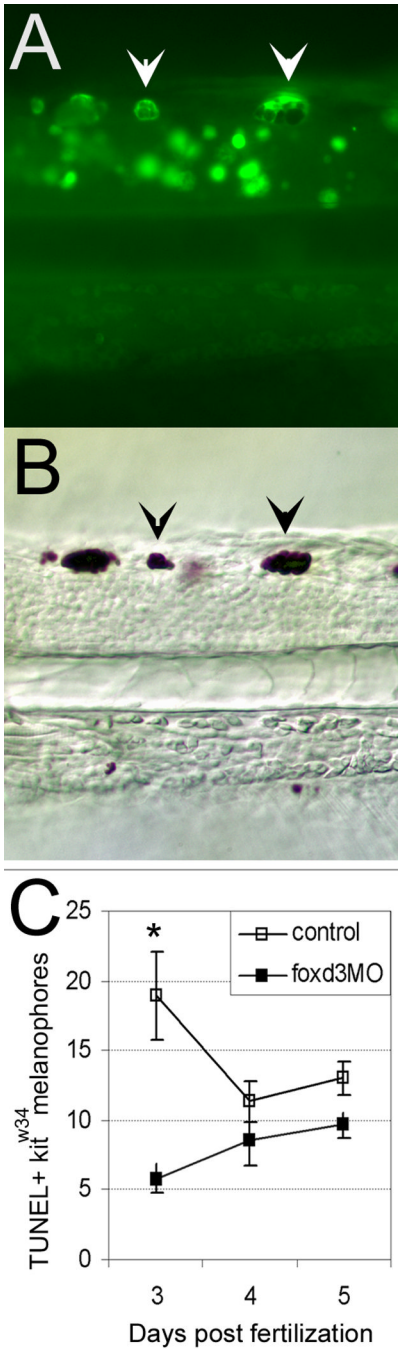

Fig. 7.

foxd3 loss-of-function partially rescues melanophores from apoptosis in *kit*^{w34} larvae. A) 3dpf *kit*^{w34} larvae analyzed by TUNEL assay. Examples of posterior trunk melanophores positive for TUNEL signal are marked with white arrowheads. B) Brightfield image of larvae shown in A. TUNEL positive melanophores (black arrowheads) are distinct in size and shape. C) Line graph indicating the total number of TUNEL positive melanophores found in the dorsal stripe of uninjected or *foxd3* MO injected *kit*^{w34} larvae quantified at 3, 4 and 5 dpf. There is a significant decrease in TUNEL positive melanophores at 3 dpf with *foxd3* loss-of-function. (control n=45 fish, 649 TUNEL+ cells; *foxd3*MO n=64 fish, 493 TUNEL+ cells; *, $p<0.001$ by Bonferroni posttest at 3dpf).

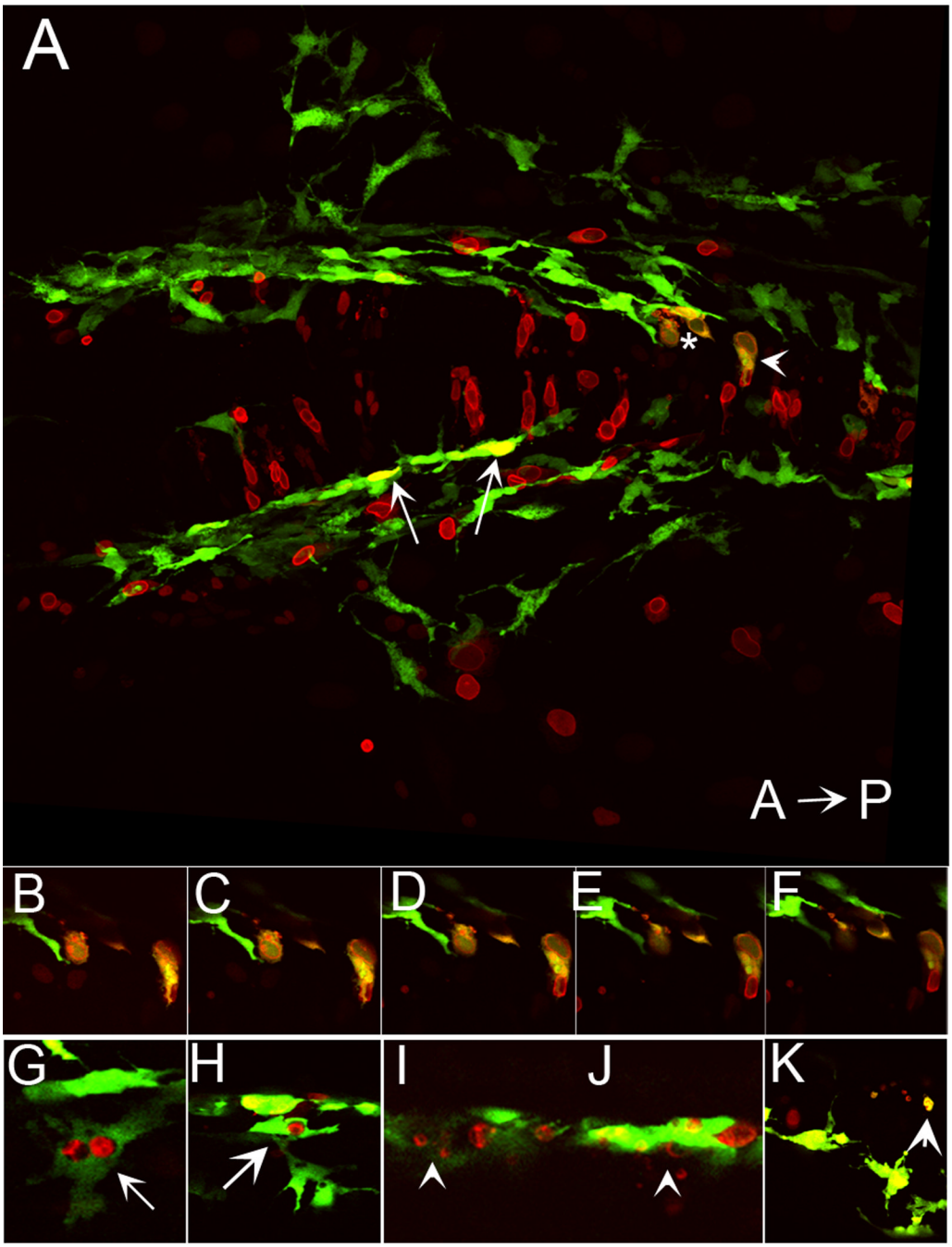

Fig. 8.

Ectopic expression of *foxd3* promotes cell death in *kit* mutants. A) Confocal stack image showing a dorsal view of posterior head of 28 hpf *kit*$^{w34/w34}$ embryo transgenic for *mi::gfp* and also expressing *myc-foxd3* (red) under the control of a heat shock promoter. Expression of *myc-foxd3* was induced at 19 hpf. Both wildtype (arrows) and fragmenting (asterisk and arrowhead) melanophores are observed. B- F) Confocal slices showing fragmenting cells indicated by asterisk and arrowhead in A. Note the presence of Foxd3 positive fragments within the GFP+ melanophores. G–H) Confocal slices showing additional examples of GFP/Foxd3+ cells designated as normal melanophores. I–J) Confocal slices showing examples of GFP/Foxd3+ cells designated as fragmenting melanophores (arrowheads).

TABLE 1

Effect of *kit*^{w34} and *foxd3*^{zdf10} loss-of-function on total melanophores

GENOTYPE	AVERAGE # TOTAL MELANOPHORES*
kit^{w34}/+	307.8 ± 42.6 (6)
kit$^{w34/w34}$	118.7 ± 41.8 (7)
kit$^{w34/w34}$; *foxd3*$^{zdf10/+}$	122.2 ± 47.6 (10)
kit$^{w34/w34}$; *foxd3*$^{zdf10/zdf10}$	176.0 ± 41.9 (10)

Larvae were fixed at 4dpf for counting.

*Melanophore averages for each genotype ± standard deviation are shown. The number of fish counted is in parentheses. There is a significant difference in the number of melanophores between *kit/foxd3* double mutants and *kit* single mutants (p,0.05 by Tukey's posthoc test after 1-way ANOVA).

TABLE 2

Effect of ectopic *foxd3* expression on melanophore morphology. Data are the numbers of cells with indicated morphology and genotype.

	Wildtype *or* kit^{w34}/+	$kit^{w34/w34}$
Fragmented	0	7
Normal	13	11

Larvae were fixed at ~28hpf and antibody stained for Foxd3 (anti-Myc) and GFP. Fish were screened for the presence of *foxd3* fragmented cells and GFP expression. Positive fish were imaged and the number of cells with the indicated morphologies were counted in the different genetic backgrounds. Distributions are significantly different (p=0.025, Fisher's exact test).